

NON RELATIVISTIC RESISTIVE WALL WAKE FIELDS AND SINGLE BUNCH STABILITY

D. Quatraro, G. Rumolo

*European Organization for Nuclear Research (CERN),
CH-1211 Genève 23, Switzerland*

Abstract

The usual approach for the resistive pipe wall assumes the beam moves with the speed of light. For many low energy rings, such as the Proton Synchrotron Booster (PBS), possible performance limitations may arise from non relativistic resistive wall wake fields. In this regime not only the head of the bunch can interact with the tail but also the vice versa holds.

In this paper we analyze numerical results showing the resistive wake field calculated from non relativistic impedance models. In addition we analyze the well known two particles model assuming that even the trailing particle can affect the leading one. We observe significant changes in the stability domain.

INTRODUCTION

Several accelerators, such as the PS booster (PSB) and the Proton Synchrotron (PS) at CERN produce intense proton beams at energies around 1 GeV. This regime is quite far from the ultra relativistic one: for the PSB a proton has $\gamma \simeq 2$ at the highest kinetic energy. For high intensity beam a possible limitation could be represented by the resistive wall impedance.

The ultra relativistic approach for the resistive wall impedance assumes the excited wake field to be zero in front of each particle. On the other hand for a low energy bunch, not only the leading particle can affect the trailing one but also the vice versa.

In literature we can find some examples which derive non ultra relativistic formulae for the resistive wall impedance [1]-[3]. In this paper we used the approach developed by Zimmermann and Oide [1] and we numerically calculated the resistive wall wake functions as inverse Fourier transform of the impedance.

In order to study possible effects on the bunch stability, we modified the so called two particle model allowing the trailing particle to effect the dynamics of the leading one and we studied the stability of the system.

THE IMPEDANCE CALCULATIONS

As we already mentioned, in order to calculate the wake fields, we start from Eq. (51) in reference [1].

$$Z_{||}(\omega) = i \frac{Z_0 c k_r^2}{2\pi\omega} [K_0(k_r r) + I_0(k_r r) \cdot \frac{\omega^2 \lambda K_1(bk_r) K_0(b\lambda) + k_r c^2 (\lambda^2 - k^2) K_0(bk_r) K_1(b\lambda)}{\omega^2 \lambda I_1(bk_r) K_0(b\lambda) - k_r c^2 (\lambda^2 - k^2) I_0(bk_r) K_1(b\lambda)}] \quad (1)$$

where c is the speed of light, $Z_0 = \mu_0 c = 120\pi\Omega$, b is the beam pipe radius, r is the radial coordinate of the test particle, I_j, K_j are the j -th order modified Bessel function and

$$\begin{cases} k_r = |\omega|/\gamma\beta c \longrightarrow k_r^2 = \omega^2/\gamma\beta c \\ \lambda^2 = -i\mu_0\sigma\omega + k_r^2 \end{cases} \quad (2)$$

σ and μ being respectively the conductivity and the permeability of the beam pipe. In the Eq. (2) we have to subtract the contribution of the direct space charge, in order to obtain the resistive wall impedance. The space charge contribute is given by

$$Z_{||}^{sc}(\omega) = i \frac{Z_0 c k_r^2}{2\pi\omega} \left[K_0(k_r r) - \frac{K_0(bk_r)}{I_0(bk_r)} I_0(k_r r) \right] \quad (3)$$

and after a little algebra we obtain

$$Z_{||}(\omega) = i \frac{Z_0 c k_r^2}{2\pi\omega} I_0(k_r r) \left[\frac{K_0(bk_r)}{I_0(bk_r)} + \frac{\omega^2 \lambda K_1(bk_r) K_0(b\lambda) + k_r c^2 (\lambda^2 - k^2) K_0(bk_r) K_1(b\lambda)}{\omega^2 \lambda I_1(bk_r) K_0(b\lambda) - k_r c^2 (\lambda^2 - k^2) I_0(bk_r) K_1(b\lambda)} \right] \quad (4)$$

which is the longitudinal resistive wall impedance for an arbitrary β . The following plots Fig. 1 show the longitudinal impedance for two different energies at the PSB.

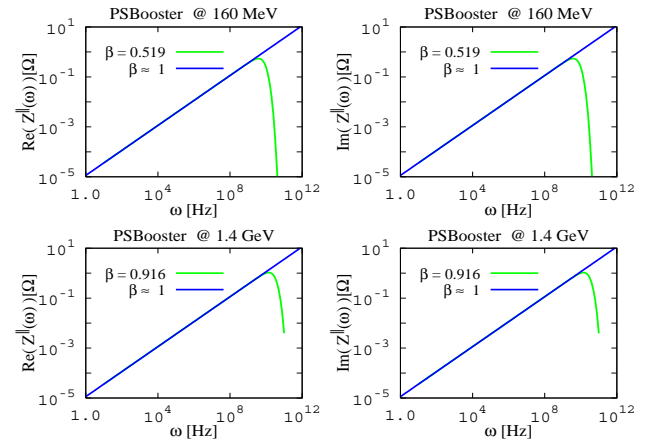


Figure 1: Comparison between the real (left) and the imaginary (right) part of the longitudinal resistive wall impedance, for ultra relativistic approach [4] (—) and non ultra relativistic one (—) Eq. (7).

In the computation of the transverse impedance, due to a more complicated expression, we used the approximation

$$Z_{\perp}(\omega) \sim \frac{2\beta c}{b^2\omega} Z_{||}(\omega) \quad (5)$$

which is always valid for the resistive wall impedance at medium and high frequency regime [4]. Fig. 2 shows the transverse resistive wall impedance starting from Eq. (4) and applying the approximation Eq. (5).

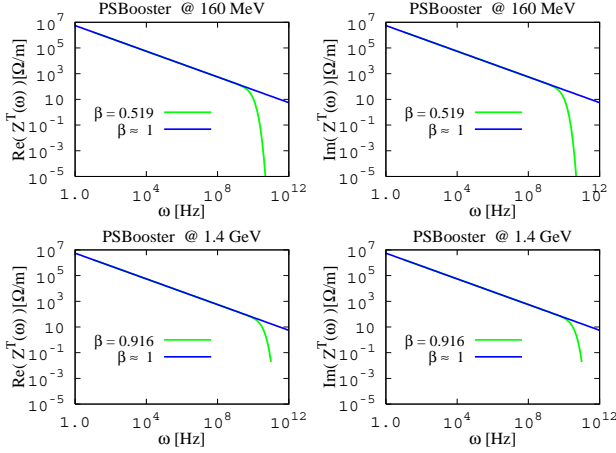


Figure 2: Comparison between the real (left) and imaginary (right) part of the transverse resistive wall impedance, for ultra relativistic approach [4] (—) and non ultrarelativistic one (—) casting Eq. (4) in Eq. (5).

In the former plots we scanned the impedance frequency up to $\omega = 10^{11}$ and we observe that the higher the β the slower is the convergence of both the real and imaginary part of the impedance to zero.

Performing the numerical Fourier transform (via the FFT algorithm) of the impedance Eq. (4) and Eq. (5) we obtaining the longitudinal and transverse wake field, $W'_0(z)$ and $W_1(z)$ respectively which are given by

$$\begin{cases} W'_0(z) = \frac{1}{2\pi} \int_{-\infty}^{+\infty} d\omega e^{i\omega z/\beta c} Z_{\parallel}(\omega) \\ W_1(z) = \frac{-i}{2\pi} \int_{-\infty}^{+\infty} d\omega e^{i\omega z/\beta c} Z_{\perp}(\omega) \end{cases} \quad (6)$$

In Fig. 3 we show the results we obtained compared against the ultra relativistic case, to which the calculated wake fields converge when $\beta \rightarrow 1$. Concerning the transverse wake field we experienced some numerical problems at low frequencies when applying the FFT algorithm. Indeed to avoid this problem we expanded Eq. (4) for the high frequency regime. Due to the fact that for $\beta < 1$ the wake functions should be continuous functions of z in the neighbourhood of $z = 0$ [5], we performed the limit of Eq. (4) as ω approaches high frequencies, which means small z . In fact to perform this limit we should consider the quantity $b|\omega|/\gamma\beta c \gg 1$ which reads $|z| \ll b/\gamma$ in z -space: these are the ranges of validity for the transverse resistive wall impedance and wake field respectively. Expanding the Bessel functions as reported in [6] we obtain the following representation of Eq. (4)

$$Z_{\parallel}(\omega) = i \frac{Z_0 \omega}{c \beta^2 \gamma^2} I_0(r|\omega|/\gamma\beta c) e^{-2b|\omega|/\gamma\beta c} \cdot \left[\frac{\sqrt{|\omega|\sigma\mu_0} (1 - i \operatorname{sgn}(\omega))}{\sqrt{|\omega|\sigma\mu_0} (1 - i \operatorname{sgn}(\omega)) + \sqrt{2} \operatorname{sgn}(\omega) c/\beta\gamma (i\mu_0\sigma + \omega/c^2)} \right] \quad (7)$$

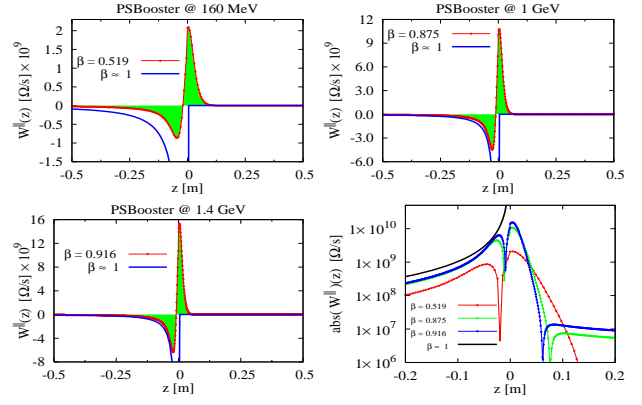


Figure 3: Comparison between the ultra relativistic (—) and the non ultra relativistic (—) longitudinal resistive wall wake field for three different energies available at PSB. The filled region (●) is the area between the non ultra relativistic wake and the $W'_0 = 0$ axis. The bottom right plot shows the comparison in log scale of the absolute value of the field for the different energies and for the ultra relativistic case.

In Fig. 4 we compare Eq. (7) against Eq. (4).

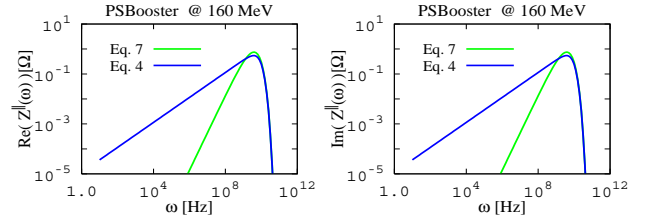


Figure 4: Comparison between Eq. (7) (—) and its approximation at high frequency Eq. (4) (—).

Applying Eq. (5) to Eq. (7) we obtain an approximation of the transverse resistive wall impedance at high frequencies. In Fig. 5 we plot the transverse resistive wall wake fields for two different energies at PSB.

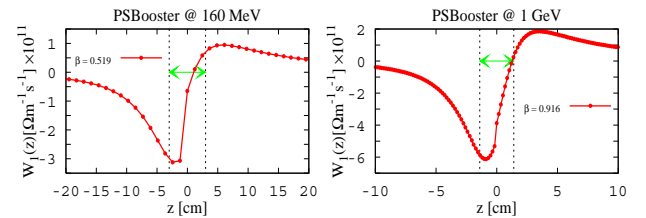


Figure 5: Transverse resistive wall wake field (—) for small distances, at two different energies. The arrow (\leftrightarrow) indicates the range of validity.

EFFECTS ON THE TRANSVERSE MODE COUPLING INSTABILITY

In order to study the mechanism of the Transverse Mode Coupling Instability (TMCI) we consider the so called two particle model, in which the bunch is described by a leading and a trailing particle having transverse displacement y_1 and y_2 respectively. They do not only oscillate transversally with a frequency ω_β but also have a synchrotron motion of frequency $\omega_s = 2\pi/T_s$. During time $t \in [nT_s; (2n+1)T_s/2]$ particle 1 leads particle 2 and vice versa during time $t \in [(2n+1)T_s/2; nT_s]$ with $n \in \mathbb{N}$. The equations of motion for the system are given by

$$\vec{\Phi} = \begin{pmatrix} x_1' \\ -(\omega_\beta/c)^2 x_1 + \alpha_1 x_2 \\ x_2' \\ -(\omega_\beta/c)^2 x_2 + \alpha_2 x_1 \end{pmatrix}, \quad \alpha_j = \frac{Nr_0 W_j}{2\gamma C}, \quad j = 1, 2, \quad (8)$$

and we solved the system $\dot{\vec{x}} = \vec{\Phi}(\vec{x})$ numerically. In writing Eq. (8) we assumed the wake fields W_j (integrated over the machine circumference C) are constant, and N represent the intensity of the bunch.

We solved Eq. (8) assuming not only the leading particle affecting the trailing one but also the contrary holds true. In Fig. 6 we plot the stability region in the $(\omega_\beta/\omega_s, \Gamma)$ plane for different values of W_1 , which is the value of the wake field that the trailing particle applies on the leading one. The quantity $\Gamma = \frac{\pi N r_0 W_2 c^2}{4\gamma C \omega_\beta \omega_s}$ gives an estimation of the bunch intensity and the wake field strengths. In partic-

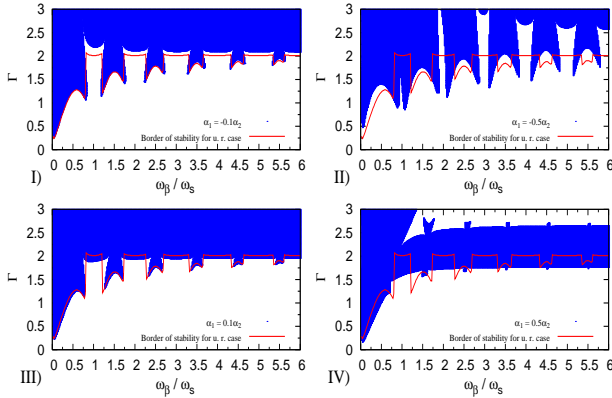


Figure 6: Stability region in the $(\omega_\beta/\omega_s, \Gamma)$ plane for the two particle beam against the TMCI. The blue dotted regions (•) are those where the system is unstable. The red line (–) stands for the border of stability of the system at the ultra relativistic regime. The values used for the simulations are: $\alpha_1 = -0.1\alpha_2$ plot I), $\alpha_1 = -0.5\alpha_2$ plot II), $\alpha_1 = 0.1\alpha_2$ plot III) and $\alpha_1 = 0.1\alpha_2$ plot IV)

ular from plot IV) of Fig. 6 we can observe that the system could becomes stable again for a fixed value of ω_β/ω_s increasing the bunch intensity. In Fig. 7 we plot the frequency spectrum of the center of charge of the beam. We observe

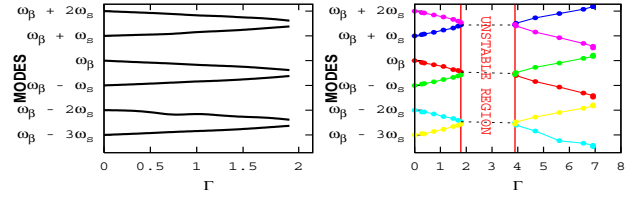


Figure 7: Frequency spectrum of the center of charge (which is $y_1 + y_2$) of the beam versus the bunch intensity. The instability occurs when the mode frequencies merge. This happens for $\Gamma \sim 2$ in the ultra relativistic case (left), and the system stays unstable. For the non ultra relativistic one (right) the system becomes unstable at $\Gamma \sim 2$ for a first time: the mode frequencies then splits for $\Gamma \sim 4$, the system returns to be stable and then unstable again for $\Gamma \sim 7$.

that the ultra relativistic case gets unstable when $\Gamma \rightarrow 2$ and remains unstable while increasing the bunch population N . On the other hand we observed the coupling ($\Gamma \sim 2$) and decoupling ($\Gamma \sim 4$) for the non ultrarelativistic case when $\alpha_1 = \alpha_2/2$.

CONCLUSIONS

We have calculated numerically the longitudinal resistive wall wake field in the non ultra relativistic regime. We have seen that the longitudinal field in front of the leading particle is not negligible. In the high-frequency/short-distances regime, we have also obtained the transverse non relativistic resistive wall wake. We can also see a change of sign in the neighbourhood of $z = 0$, for the longitudinal and the transversal wake fields.

In addition we have simulated with a simple model the possible affects on the TMCI, considering a nonzero wake when $z > 0$. We studied in the details the spectrum of the bunch center of charge in the case of a coupling and decoupling of the modes with increasing the bunch intensity.

REFERENCES

- [1] F. Zimmermann and K. Oide, PRLSTAB **7**, 044201 (2004)
- [2] A. M. Al-khateeb, O. Boine-Frankenheim, I. Hofmann, and G. Rumolo, Phys. Rev. E **63**, 026503 (2001)
- [3] E. Métral, B. Salvant, B. Zotter, CERN-LHC-Project-Report 1014
- [4] A. Chao, *Physics of Collective Beam Instabilities in High-Energy Accelerators* (Wiley, New York, 1993)
- [5] L. Palumbo, V. G. Vaccaro and M. Zobov *Wake fields and impedance* LNF-94-041-P- Frascati Naz. Lab., 1994
- [6] M. Abramowitz and I.A. Stegun, Natl. Bur. Stand. Appl. Math. No.55(U.S. GPO, Washington, DC, 1970)